MOLECULAR AND CELLULAR BIOLOGY, Sept. 2004, p. 7456–7468 Vol. 24, No. 17
0270-7306/04/$08.00+0 DOI: 10.1128/MCB.24.17.7456–7468.2004

MUC20 Suppresses the Hepatocyte Growth Factor-Induced Grb2-Ras Pathway by Binding to a Multifunctional Docking Site of Met

Toshio Higuchi,[1]† Takuya Orita,[1]† Ken Katsuya,[1] Yoshiki Yamasaki,[1] Kiyotaka Akiyama,[1] Huiping Li,[2] Tadashi Yamamoto,[2] Yutaka Saito,[1] and Motonao Nakamura[1]*

Central Pharmaceutical Research Institute, Pharmaceutical Frontier Research Laboratories, Japan Tobacco Inc., Yokohama,[1] and Institute of Nephrology, Faculty of Medicine, Niigata University, Niigata,[2] Japan

Received 11 March 2004/Returned for modification 30 April 2004/Accepted 29 May 2004

A cDNA encoding a novel mucin protein, MUC20, was isolated as a gene that is up-regulated in the renal tissues of patients with immunoglobulin A nephropathy. We demonstrate here that the C terminus of MUC20 associates with the multifunctional docking site of Met without ligand activation, preventing Grb2 recruitment to Met and thus attenuating hepatocyte growth factor (HGF)-induced transient extracellular signal-regulated kinase-1 and -2 activation. Production of MUC20 reduced HGF-induced matrix metalloproteinase expression and proliferation, which require the Grb2-Ras pathway, whereas cell scattering, branching morphogenesis, and survival via the Gab1/phosphatidylinositol 3-kinase (PI3K) pathways was not affected. Thus, MUC20 reduces HGF-induced activation of the Grb2-Ras pathway but not the Gab1/PI3K pathways. We further demonstrate that the cytoplasmic domain of MUC20 has the ability to oligomerize and that the oligomerization augments its affinity for Met. Taken together, these results suggest that MUC20 is a novel regulator of the Met signaling cascade which has a role in suppression of the Grb2-Ras pathway.

Hepatocyte growth factor (HGF), a multifunctional polypeptide produced in liver, kidney, and various other tissues, elicits a broad spectrum of biological activities, including mitogenesis, morphogenesis, and survival. All of these responses are mediated by a single receptor, Met, which belongs to the tyrosine kinase receptor superfamily. HGF is highly produced in mesenchymal or stromal cells but not in epithelial cells, whereas Met is expressed predominately in cells of epithelial origin. HGF signaling through Met depends on a multifunctional docking site (MDS) located in the C terminus of the receptor, comprising two phosphotyrosine residues within the sequence Y^{1349}VHVNATY^{1356}VNV. Upon phosphorylation of these tyrosine residues, this sequence interacts with several signal transducers and adaptors, such as phosphatidylinositol 3-kinase (PI3K), Gab1, and Grb2. Following the recruitment of these factors onto the MDS, biological responses are elicited by the Grb2-Ras and Gab1/PI3K pathways, with the former being required for proliferation and the latter being required for survival, scatter, and morphogenesis.

Aberrant activation of Met signaling is likely to contribute to the generation and progression of multiple types of tumors and metastases; therefore, tight regulation could be necessary for these pathways. One proposed mechanism is that inactivation of Met signaling is promoted by phosphorylation of a critical serine residue (Ser^{985}), located in a juxtamembrane domain of Met. This phosphorylation of Ser^{985}, modulated by Met-recruited phospholipase C-γ, results in down-regulation of tyrosine autophosphorylation of Met (4). Another proposed mechanism for desensitization is receptor degradation mediated by polyubiquitination. Cbl, which is known as a proto-oncogene product, has been determined to be a common negative regulator, inducing polyubiquitination of Met and other tyrosine kinase receptors. Recruitment of Cbl to the phosphotyrosine residue within the juxtamembrane of Met is promoted by MDS-associated Grb2 (20). Subsequently, Cbl rapidly interacts with both CIN85 and endophilins to form a regulatory complex, and then this complex mediates the internalization of the recognized receptors (21). All of these regulatory events are involved in the late signaling phase, namely, desensitization of the Met signaling cascade. Other mechanisms, however, by which Met-associated factors selectively suppress either the Grb2-Ras or the Gab1/PI3K pathways have not yet been reported.

In kidney, the Met signaling cascade is implicated not only in renal development and maintenance of kidney functions but also in tubular repair and regeneration under various normal and pathological conditions. In animal models of chronic renal disease, endogenous HGF prevents the progression of tissue fibrosis and renal dysfunction by suppressing the expression of transforming growth factor β, a pathogenic mediator in tissue fibrosis (16). Recent studies have revealed that endogenous HGF production is augmented after toxic or ischemic acute renal injury, and exogenous HGF can enhance regeneration and remodeling of the tissues by promoting mitogenesis, cell migration, morphogenesis, and cell survival (15, 17). Thus, several experimental models suggest that HGF could be a potent therapeutic agent with a remarkable ability to ameliorate renal injury and fibrosis by enhancing cell survival and tissue regeneration.

Recently, we obtained a novel mucin protein, MUC20, containing serine-, threonine-, and proline-rich repeats in its extracellular domain (6). The mRNA of MUC20 is highly expressed in kidney, and the expression is up-regulated in the kidneys of patients with immunoglobulin A nephropathy, in an

* Corresponding author. Mailing address: Central Pharmaceutical Research Institute, Pharmaceutical Frontier Research Laboratories, Japan Tobacco Inc., Yokohama, 236-0004, Japan. Phone: 81-45-786-7693. Fax: 81-45-786-7692. E-mail: motonao.nakamura@ims.jti.co.jp.

† T.H. and T.O. contributed equally to this work.

animal model of lupus nephritis, and in mice with acute renal injury caused by cisplatin administration or unilateral ureteral obstruction. Thus, regulators of MUC20 function and/or expression may be useful therapeutics for treating the development and progression of renal diseases. Here, to clarify the physiological and pathological functions of MUC20, we identified associated proteins by a yeast two-hybrid screen. MUC20 was shown to associate with Met and was further found to regulate the Met signaling cascade. We show that the interaction between MUC20 and Met prevents Grb2 recruitment to HGF-activated Met and attenuates the resulting transient extracellular signal-regulated kinase-1 and -2 (ERK1/2) activation in the Grb2-Ras pathway, impairing the HGF-induced biological effects that require the Grb2-Ras pathway without affecting the Gab1/PI3K pathways. Understanding of the cellular events elicited by HGF in epithelia, including our findings, should provide significant clues to mechanisms important for such complex biological processes as development and regeneration following acute injury.

MATERIALS AND METHODS

Yeast two-hybrid screening. We used the Matchmaker GAL4 yeast two-hybrid system 3 (Clontech). As baits, DNA fragments encoding MUC[439-503] and MUC[381-503] were cloned into pGBKT7. Each plasmid was transformed into yeast strain AH109 along with prey plasmids of a human kidney cDNA library (pADKT7). Transformants grown on SD plates lacking Leu, Trp, and His were patched onto freshly prepared SD plates lacking Leu, Trp, and His; SD plates lacking Leu, Trp, and Ade; and SD plates lacking Leu and Trp with 5-bromo-4-chloro-3-indolyl-β-D-galactopyranoside to select positive clones.

Plasmids and cell transfections. The plasmids phMUC20, phMUC20(Flag), phMUC20(His), phMUC20[ΔC53], pmMUC20, pmMUC20[ΔC53], pMUC[244-345], pMUC[244-380], pMUC[244-415], and pMUC[244-450] were constructed by cloning human MUC20, C-terminal Flag-tagged human MUC20, C-terminal His-tagged human MUC20, human MUC20 with a truncation of the C-terminal 53 residues, mouse MUC20, mouse MUC20 with a truncation of the C-terminal 53 residues, and human MUC20 fragments (residues 244 to 345, 244 to 380, 244 to 415, and 244 to 450) into pcDNA3 (Invitrogen), respectively. The human HGF (hHGF) expression plasmid, phHGF, was purchased from Invitrogen. To generate β-galactosidase mutant-fused constructs MUC/Δω, MUC/Δα, MUC[ΔC53]Δω, and MUC[ΔC53]Δα, DNA fragments for the Δα and Δω mutants of β-Gal were prepared by PCR with genomic DNAs of *Escherichia coli* strains DH5α and DH5 as templates, respectively, and then MUC20 and MUC[ΔC53] were fused with the Δα or Δω mutants, respectively, and then cloned into pcDNA3. For Met/Δα and Met[C91]/Δα, DNA fragments encoding full-length Met and the C-terminal 91 residues of Met were fused with the Δα mutant and then cloned into pcDNA3. The eFas/cMUC20 plasmid was constructed by cloning a chimeric fragment, consisting of the mouse Fas (residues 1 to 205) and the human MUC20 (residues 213 to 503), into pcDNA3. The eFas/cMUC20/Δα and eFas/cMUC20/Δω plasmids were prepared by fusion of the Δα and Δω fragments with the C terminus of the eFas/cMUC20. HEK293 and CHO-K1 cells were purchased from the American Type Culture Collection and grown as recommended for each cell line. Cells were transfected by using GeneJammer reagent (Stratagene).

Immunoprecipitation and immunoblotting. Cells starved for 16 h in serum-free medium were stimulated with either 20 ng of HGF (Calbiochem) per ml or 100 ng of epidermal growth factor (EGF) (Peprotech) per ml for 5 min at 37°C and then were suspended in lysis buffer (1% NP-40, 137 mM NaCl, 10% glycerol, 1 mM Na_3VO_4, and 20 mM Tris-HCl [pH 8.0]) containing protease inhibitors (1 mM phenylmethylsulfonyl fluoride, 0.2 trysin inhibitory units of aprotinin per ml. and 20 μg of leupeptin per ml). For immunoprecipitations, aliquots of the lysates (200 μg of protein) were incubated on a rotating wheel at 4°C for 1 h with the appropriate antibody. The precipitates, collected on protein G-coupled Sepharose beads (Amersham-Pharmacia Biotech), were resuspended in sodium dodecyl sulfate sample buffer and heated at 95°C for 3 min. The immunoprecipitates or total cell lysates (10 μg of proteins) were analyzed by sodium dodecyl sulfate-polyacrylamide gel electrophoresis, followed by immunoblotting with primary antibodies and horseradish peroxidase-conjugated secondary antibodies, and specific bands were detected with an ECL system (Amersham-Pharmacia Biotech). The following antibodies were used: anti-human MUC20 (6), anti-Met (C-28; Santa Cruz), anti-poly(His) (H-15; Santa Cruz), anti-Gab1 (H-198; Santa Cruz), anti-Grb2 (C-23; Santa Cruz), anti-Flag (M2; Sigma), anti-ERK (p44/42 mitogen-activated protein kinase [MAPK]; Cell Signaling), anti-p-ERK (phospho-p44/42 MAPK; Cell Signaling), anti-Akt (Cell Signaling), anti-p-Akt (phospho-Akt [Ser^{473}]; Cell Signaling), anti-p-tyrosine (P-Tyr-100; Cell Signaling), and anti-mFas (mouse Fas/TNFRSF6 [R&D Systems], RK-8 [MBL], and RMF6 [MBL]).

Immunohistochemistry. Normal renal samples were obtained, with informed consent, from nephrectomized kidneys bearing renal tumors. They were fixed with methyl-carnoy fixative, embedded in paraffin, and sectioned. After being dewaxed with xylene and dehydrated with graded ethanol solutions, they were incubated with anti-human MUC20 (1 μg/ml), anti-human Met (Santa Cruz; 0.1 μg/ml), or anti-human aquaporin-1 (AQP1) (Santa Cruz; 0.1 μg/ml) as the first antibody and anti-rabbit immunoglobulins conjugated to peroxidase-labeled dextran polymer (EnVison; DAKO) as the second antibody. The peroxidase reaction products were visualized by the standard immunoperoxidase technique.

β-Gal activity. Cells cultured in white 96-well plates were lysed by addition of GAL-Screen substrate (Tropix PE Biosystems) and incubated at room temperature for 1 h. Luminescence was measured with a MicroLumat Plus instrument (EG & G Berthold).

Reverse transcription-PCR (RT-PCR). Cells cultured in the presence or absence of 2 μg of doxycycline (DOX) per ml were starved for 16 h in serum-free medium prior to stimulation with 20 ng of HGF per ml for 3 h. Reverse transcription of total RNAs prepared from these cells was carried out by using an Advantage RT-for-PCR kit (Clontech). PCR was performed for 30 cycles as follows: denaturation at 95°C for 30 s, annealing at 55°C for 30 s, and extension at 72°C for 2 min. The primer sets were as follows: for the human matrix metalloproteinase 1 (MMP-1) mRNA, 5′-CATCCAAGCCATATATGGACGT TCC-3′ and 5′-TCTGGAGAGTCAAAATTCTCTTCGT-3′, and for the human MMP-9 mRNA, 5′-GGCATCCGGCACCTCTATGGTCC-3′ and 5′-GCCACT TGTCGGCGATAAGGAAGG-3′. The primers used for GAPDH (glyceraldehyde-3-phosphate dehydrogenase) mRNA were purchased from Clontech.

Scattering and branching tubulogenesis assays. Cells cultured in the presence or absence of 2 μg of DOX per ml were plated in Dulbecco's modified Eagle's medium containing 10% serum in a six-well plate. Cells were allowed to attach for at least 4 h, and 20 ng of HGF per ml, 10 μM LY294002 (Cell Signaling), and 2 μg of DOX per ml were added as indicated. Photographs were taken 48 h after stimulation. Formation of branched tubules was analyzed by using a 3D Collagen Cell Culture System (Chemicon). Cells cultured in the presence or absence of 2 μg of DOX per ml were harvested, suspended at a final concentration of 1,000 cells/ml in a collagen solution, and dispensed in 96-well plate. After 1 h, 100 ng of HGF per ml, 10 μM LY294002, and 2 μg of DOX per ml were added as indicated. After 7 days, the branching tubulogenesis responses were evaluated.

Apoptosis assay. Cells were pretreated with 10 μM U0126 or 10 μM LY294002 (Cell Signaling) for 2 h before stimulation with 20 ng of HGF per ml for 24 h, followed by addition of 100 ng of an agonistic anti-Fas antibody (CH-11; Medical & Biological Laboratories) per ml. After 48 h of treatment, the fraction of cells undergoing apoptosis was quantified by measuring the amount of free nucleosomes from these cells by using a Cell Death Detection $ELISA^{PLUS}$ kit (Roche Diagnostics).

Generation of MUC20-transgenic (MUC20-Tg) mice. Mouse MUC20 cDNA (6) was expressed under the control of the chicken β-*actin* promoter on pCAGGS (19). The purified fragment containing the MUC20 gene was dissolved in injection buffer (0.25 mM EDTA and 10 mM Tris-HCl [pH 7.5]) at 5 μg/ml and injected into the pronuclei of fertilized eggs from superovulated ICR females (Charles River Japan) mated with ICR males. For genotyping, genomic DNAs were isolated from tail biopsies, followed by PCR analysis with primers specific to the vector sequence (5′-TAATCAATTACGGGGTCATTAGTTCA TAGC-3′ and 5′-TCCCATAAGGTCATGTACTGGGCATAATGC-3′). Expression of the transgene in several tissues, including liver, kidney, brain, heart, and muscle, but not lung, was confirmed by Northern blotting as described previously (reference 6 and data not shown).

Preparation and growth assay of primary cells. From the kidneys of MUC20-Tg and non-Tg littermate mice (male, 8 weeks old, 27 to 34 g of body weight), primary cultures of renal tubular cells were prepared as described previously (14). Those cells, cultured in 96-well plates, were starved for 16 h prior to stimulation with or without the indicated amounts of HGF for 24 h. Cell numbers were quantified by using Cell Count Reagent SF (Nacalai Tesque).

Hydrodynamic gene transfer. A hydrodynamic gene transfer technique was used in these experiments (29). Briefly, the plasmid DNAs, phHGF (30 μg) for Tg and non-Tg mice (female, 8 weeks old, 27 to 34 g of body weight) and phHGF (50 μg) along with either pmMUC20, pmMUC20[ΔC53], or pcDNA3 (50 μg

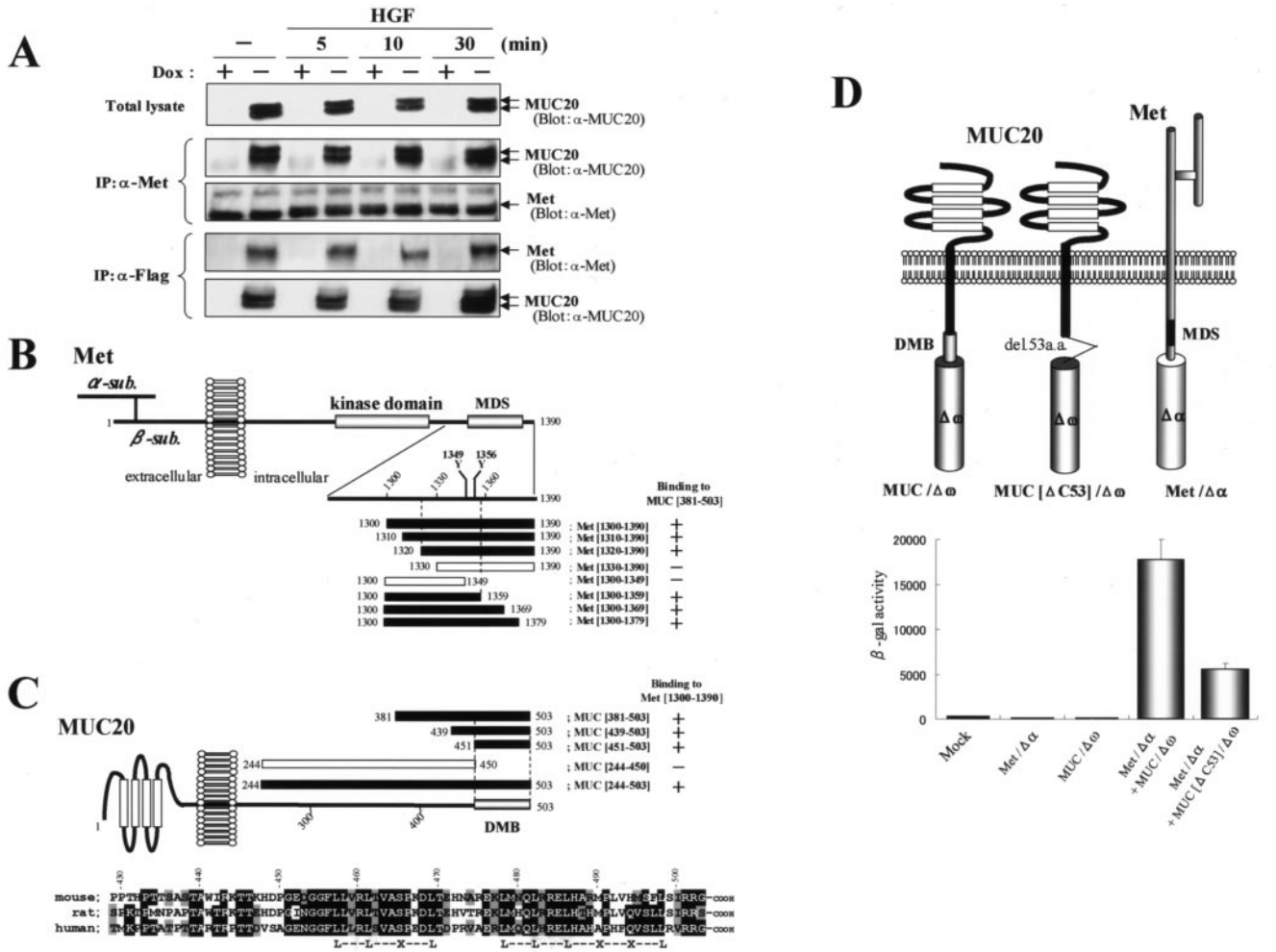

FIG. 1. Interaction of MUC20 with Met. (A) Coimmunoprecipitation of MUC20 with Met. Lysates of cells transfected with a Flag-tagged MUC20 gene were subjected to immunoprecipitation (IP) with anti-Met (α-Met) or anti-Flag antibodies, and the precipitates were immunoblotted with the indicated antibodies. Two bands representing the MUC20 proteins were detected due to posttranslational modification (6). (B) MUC20 binding domain in Met. Peptides with progressive deletions from the N- or C-terminal end of Met[1300-1390] were used for prey. Positive or negative association of each peptide with the bait peptide, MUC[381-503], in the two-hybrid assay is indicated as + or −, respectively. The domain structure of Met is also shown (2). (C) Upper panel, Met binding domain in MUC20. Positive or negative association of each cytoplasmic peptide of MUC20 to Met[1300-1390] is shown as + or −, respectively. Lower panel, alignment of the C termini of human, rat, and mouse MUC20 proteins. Residues identical in human MUC20 and the other sequences are shown by reverse type, and conservative charges are shown by gray shading. Conserved leucine repeats are indicated at the bottom. (D) Evaluation of MUC20-Met binding by using the β-Gal mutant system. Upper panel, schematic representation of three chimeric constructs. Lower panel, β-Gal activities in the transfected CHO-K1 cells. Plasmids transfected into CHO-K1 cells are indicated below each bar. Data represent means ± standard deviations ($n = 3$). (E) Immunohistochemical analysis of MUC20 and Met in human kidney. Kidney sections were stained with anti-MUC20 (a), anti-Met (b), or anti-AQP1 (c) antibodies. G, glomerulus; DT, distal tubule; PT, proximal tubule.

each) for ICR mice (male, 8 weeks old, 31 to 36 g of body weight), were diluted in 2.5 ml of saline and injected via the tail vein into circulation within 5 s. Plasma samples were collected 24 h after injection, and plasma hHGF was quantified by using an hHGF immunoassay kit (Genzyme Techne). Expression in the liver of hHGF, mouse MUC20, and MUC20[ΔC53] mRNAs derived from the injected plasmids was confirmed by RT-PCR at 24 h after injection (data not shown). Primer sets used for the RT-PCR were as follows: for the hHGF mRNA, 5′-TAATACGACTCACTATAGGG-3′ and 5′-AAAAAGCTGTGTTCGTGT GGT-3′, and for the mouse MUC20 and MUC20[ΔC53] mRNAs, 5′-GGATC AACAATGGGAGAAACA-3′ and 5′-ATTTAGGTGACACTATA-3′.

RESULTS

The C terminus of MUC20 binds to the MDS of Met. To elucidate the role of MUC20, we searched a human kidney cDNA library for proteins interacting with human MUC20 by a yeast two-hybrid screen. Since the C terminus of MUC20 is highly conserved across mammalian species, we chose as baits the two peptides MUC[439-503] (residues 439 to 503) and MUC[381-503] (residues 381 to 503). The screen yielded two peptides corresponding to the C terminus of Met, residues 1302 to 1390 (Met[1302-1390]) and 1300 to 1390 (Met[1300-1390]), both including the MDS domain. Next, to test the binding of MUC20 to Met, immunoprecipitation experiments were performed with HEK293 cells with regulatable MUC20 expression. The cells, HEK/*tet*-MUC20 cells, express C-terminally Flag-tagged human MUC20 under control of a *tet* pro-

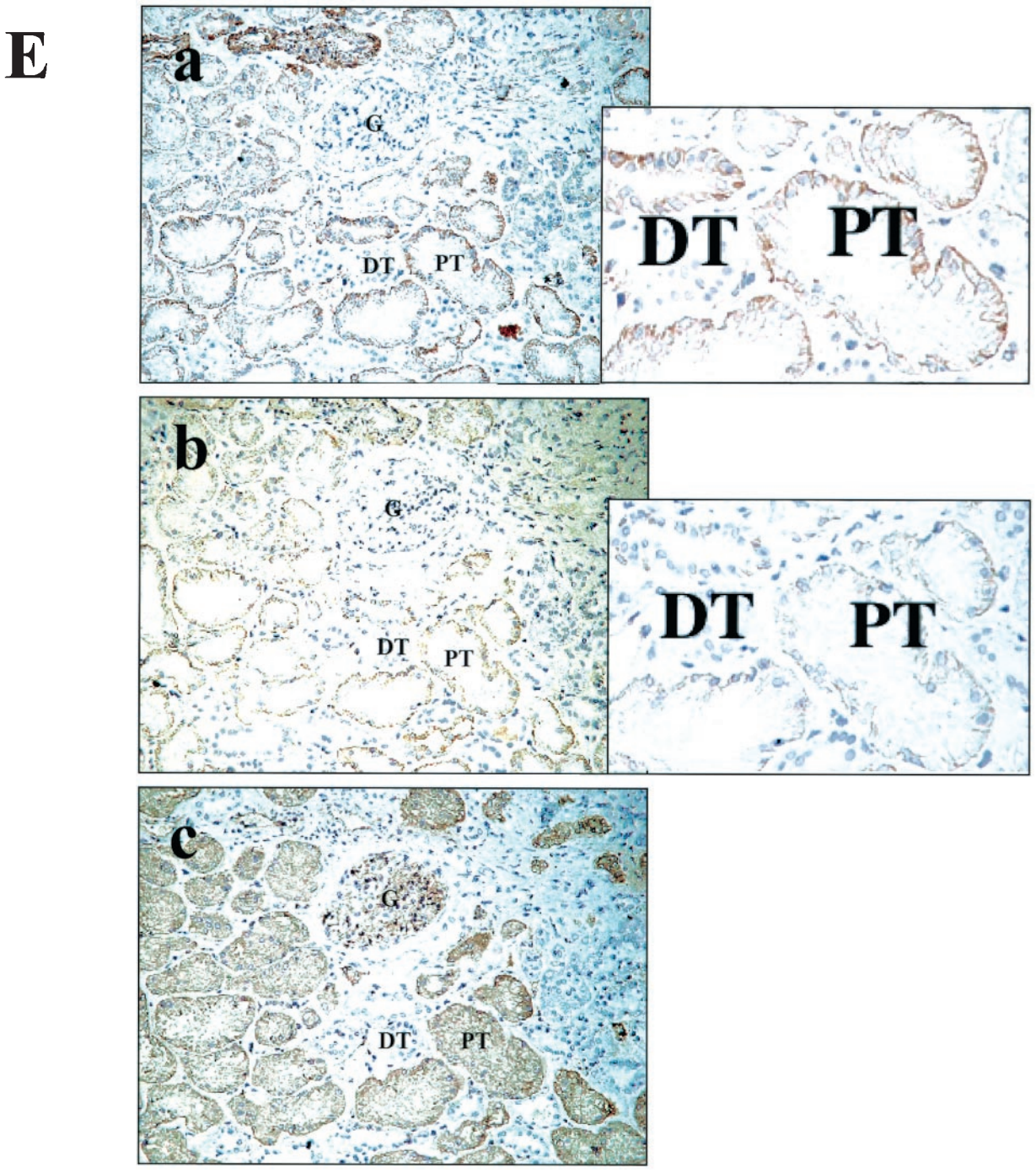

FIG. 1—*Continued*

moter, and expression of MUC20 was induced by reduction of DOX levels in the medium (6). As shown in Fig. 1A, MUC20 produced in HEK/*tet*-MUC20 cells was coimmunoprecipitated with endogenous Met. Interestingly, similar amounts of the precipitated MUC20 were observed regardless of whether these cells were stimulated with HGF, i.e., without dimerization and autophosphorylation of Met, suggesting that the activation of Met cannot be required for the MUC20-Met binding.

To clarify the domain in Met that is pivotal for binding to MUC20, several fragments of Met[1300-1390] were tested for the ability to bind MUC[381-503] in a two-hybrid assay. Recognition by the C terminus of MUC20 required the region between residues 1320 and 1359, which includes the Y^{1349}VHVNATY^{1356}VNV sequence (Fig. 1B). To clarify the domain of MUC20 involved in Met binding, we generated various fragments of the MUC20 cytoplasmic domain and then

evaluated binding of each peptide to Met[1300-1390]. Of these fragments, all peptides containing the C-terminal end, i.e., MUC[381-503], MUC[439-503], MUC[451-503], and MUC [244-503], were found to bind with Met[1300-1390], whereas MUC[244-450], which lacks the C-terminal 53 residues, did not bind, suggesting the importance of the C terminus for the Met binding (Fig. 1C, upper panel). Comparison of the sequence of human MUC20 to those of mouse and rat cognates reveals that the predicted Met binding domain is highly conserved, especially the C-terminal 53 residues, which have 79 and 81% similarity to rat and mouse proteins, respectively (Fig. 1C, lower panel). The MUC20-Met binding was also demonstrated for the mouse cognates (data not shown), suggesting a common feature of this association among mammalian species. Interestingly, we found conserved leucine residues repeated at four-residue intervals, raising the possibility that these repeats are involved in the binding to Met. The importance of the MUC20 C terminus for the Met binding was further tested by using a complementation system of β-Gal mutants (β-Gal mutant system) (24). Both full-length MUC20 and a form with the C-terminal 53 residues truncated, MUC20[ΔC53], were fused to the Δω type of β-Gal mutant, while full-length human Met was fused to the Δα type, resulting in the generation of three chimeric constructs, MUC/Δω, MUC[ΔC53]/Δω, and Met/Δα (Fig. 1D). Coexpression of MUC/Δω and Met/Δα gave rise to strong β-Gal activity, but replacement of MUC/Δω with MUC[ΔC53]/Δω caused a reduction in this activity. Combined, all of these results imply that the C terminus of MUC20, mainly the 53 terminal residues, could be crucial for binding to the MDS. Thus, we termed this region the domain for Met binding (DMB).

Marked expression of the MUC20 mRNA in the proximal tubules of the kidney was previously demonstrated by in situ hybridization (6). The proximal tubules have also been shown to produce Met intensively (3). Therefore, we examined the colocalization of both proteins in the kidney by immunohistochemistry with anti-MUC20 and anti-Met antibodies. Proximal tubules were identified by the presence of AQP1. The results, shown in Fig. 1E, revealed that immunoreactivity for both MUC20 and Met was localized in the proximal tubules, specifically in the brush border and basolateral membrane, but not in the glomeruli, distal tubules, and other sites. At a high magnification, both MUC20 and Met immunoreactivities were observed in the basal membranes of proximal tubular epithelia, indicating that both proteins are capable of associating with the membrane.

ERK1/2 phosphorylation via Met activation is reduced by MUC20 binding. We next investigated whether MUC20-Met binding affects cell signaling evoked by HGF. Following stimulation of HEK/*tet*-MUC20 cells with HGF or EGF, endogenous Met or EGF receptor, respectively, was autophosphorylated, whether or not MUC20 was produced (Fig. 2A). In the EGF-stimulated cells, phosphorylation of ERK1/2 was not affected by the production of MUC20. Indeed, in the two-hybrid assay, the C-terminal peptide of MUC20, MUC[451-503], did not bind to the EGF receptor C terminus (143 residues, including the critical domain for signaling). In contrast, HGF-evoked ERK1/2 phosphorylation was significantly decreased in the presence of MUC20. The amount of MUC20 in these cells was regulated by DOX concentration, and the suppressive effect of MUC20 on ERK1/2 phosphorylation was validated in a dose-dependent manner (Fig. 2B). ERK1/2 phosphorylation kinetics were also investigated in a time course experiment. As shown in Fig. 2C, in the absence of MUC20, the phosphorylation of ERK2 evoked by HGF showed a peak at 30 min of 14-fold over the basal level and then decreased to 2-fold over the basal level, and the phosphorylation persisted for at least 4 h after HGF stimulation. Production of MUC20 decreased the activation of ERK2 at early time points (4.5-fold), although the duration was comparable to that observed without MUC20 production. To test the possibility that the reduction in ERK1/2 phosphorylation was due to the interaction between MUC20 and Met, we examined whether MUC20[ΔC53] could still inhibit the ERK1/2 phosphorylation. MUC20[ΔC53] inhibited the phosphorylation significantly less than did full-length MUC20 (Fig. 2D), suggesting that the reduction in HGF-induced transient ERK1/2 activation might be due to the specific binding of the DMB in MUC20 to Met.

To test possible mechanisms by which MUC20 suppresses HGF-induced transient activation of ERK1/2 within the Met complex, we asked whether the association between MUC20 and Met affects the recruitment of Gab1 and Grb2 to Met. To this end, we performed immunoprecipitation experiments with anti-Gab1, anti-Grb2, and anti-Met antibodies. As shown in Fig. 2E, anti-Met antibody precipitated the same amounts of Gab1 with or without MUC20 production, indicating that MUC20 did not affect Gab1 recruitment to the activated Met. However, the precipitation of Grb2 with the anti-Met antibody was decreased in the MUC20-producing cells compared to the nonproducing cells. A similar reduction in the Grb2 recruitment was observed in a reverse experiment, i.e., immunoprecipitation with anti-Gab1 or anti-Grb2 antibody followed by blotting with anti-Met antibody (Fig. 2E). These results indicate that recruitment of Grb2, but not Gab1, could be impaired by the MUC20-Met binding, leading to the attenuation of the HGF-induced Grb2-Ras pathway.

Effects of MUC20 on HGF-induced biological responses. To gain further insight into the role of MUC20, we investigated the effects of the MUC20-Met binding on HGF-induced biological phenomena. First, we tested whether the MUC20-Met binding leads to reduced expression of MMP-1 and MMP-9, because HGF has been shown to induce the production of MMPs through the Grb2-Ras pathway (30). Indeed, both the phosphorylation of ERK1/2 evoked by HGF and the resulting induction of MMP-1 mRNA were attenuated by treatment with U0126, a specific inhibitor of MAPK/ERK kinase (data not shown). Expression of both MMP-1 and MMP-9 mRNAs, which were enhanced until 3 h after HGF stimulation, was decreased by production of MUC20, suggesting that the upregulation of MMP-1 and MMP-9 is impaired by the MUC20-Met binding (Fig. 3A).

Next, we investigated whether MUC20 affects cell scattering and branching morphogenesis by HGF. To this end, MDCK/*tet*-MUC20 cells, in which expression of human MUC20 is induced by reduction of DOX, were generated (6). In these cells, HGF-evoked ERK1/2 phosphorylation was significantly decreased in the presence of human MUC20, as well as in HEK/*tet*-MUC20 cells (data not shown). As shown in Fig. 3B, treatment with the specific PI3K inhibitor LY294002 decreased cell detachment, typical scatter activity, and the for-

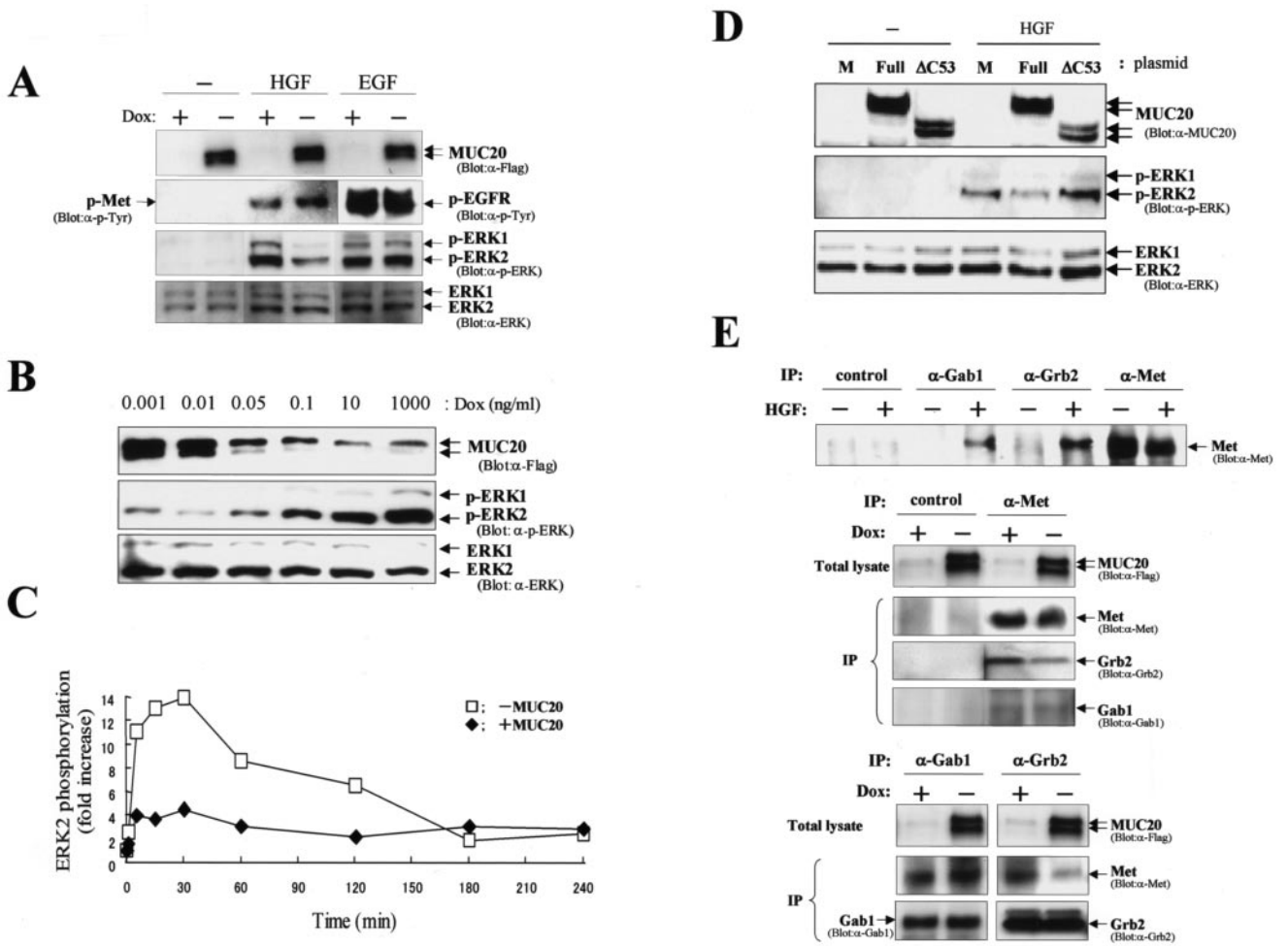

FIG. 2. MUC20 attenuates HGF-induced ERK1/2 phosphorylation. (A) Attenuation of HGF-induced ERK1/2 phosphorylation by MUC20. HEK/*tet*-MUC20 cells cultured in the presence or absence of DOX were stimulated with HGF (20 ng/ml) or EGF (100 ng/ml). The lysates from those cells were used for immunoblotting with the indicated antibodies. p, phosphorylated; α-, anti-. (B) Dose-dependent effect of MUC20 on ERK1/2 phosphorylation. Cells cultured with various concentrations of DOX were stimulated with HGF. Equivalent amounts of the cell lysates were used for immunoblotting with the indicated antibodies. (C) Activation profile of ERK2 elicited by HGF with or without MUC20 production. Cell lysates were analyzed by immunoblotting with anti-ERK and anti-p-ERK antibodies. The signal intensity for the phospho-ERK2 bands was measured by densitometry, and the intensity of each signal was normalized against that of the protein band detected with anti-ERK antibody. (D) Involvement of the DMB in the suppressive effect of MUC20. HEK293 cells transfected with either phMUC20 (Full), phMUC20[ΔC53] (ΔC53), or pcDNA3 vector (M) were stimulated with HGF and then subjected to immunoblotting with the indicated antibodies. (E) Effects of MUC20 on Gab1 and Grb2 recruitment to activated Met. Immunoprecipitation (IP) with the indicated antibodies was carried out on lysates from HGF-stimulated HEK/*tet*-MUC20 cells with or without MUC20 production. The precipitates were used for immunoblotting with the indicated antibodies.

mation of ramified tubules elicited by HGF, consistent with previous reports that the PI3K pathway is involved in these phenomena (9). In these cell scatter and branching morphogenesis experiments, no differences were observed between the MUC20-producing and -nonproducing cells. Furthermore, the effect of MUC20 on the survival activity of HGF against Fas-induced apoptosis, for which it has been reported that the Gab1/PI3K pathways are required (28), was examined in HEK/*tet*-MUC20 cells. As previously reported, in the MUC20-nonproducing cells, apoptosis evoked by an agonistic anti-Fas antibody was effectively inhibited by HGF, and this inhibition was impaired by treatment with LY294002 but not by treatment with U0126 (Fig. 3C). Under every condition tested in these experiments, no differences in cell survival were detected between the MUC20-producing and -nonproducing cells. These results, taken together, suggest that the MUC20-Met binding does not affect the part of the HGF-induced signaling cascade, possibly the Gab1/PI3K pathways, involved in cell scattering, branching morphogenesis, and cell survival.

There is evidence that transient activation of ERK1/2 stimulates proliferation; therefore, we examined whether the proliferation promoted by HGF is attenuated by MUC20. In the MUC20-producing cells used in the experiments described above, it was difficult to see the proliferative effect of HGF due to their accelerated growth, even if those cells were starved prior to the stimulation. Therefore, two strains of MUC20-Tg mice were generated to prepare primary cells. These mice developed normally and had no apparent phenotypic abnor-

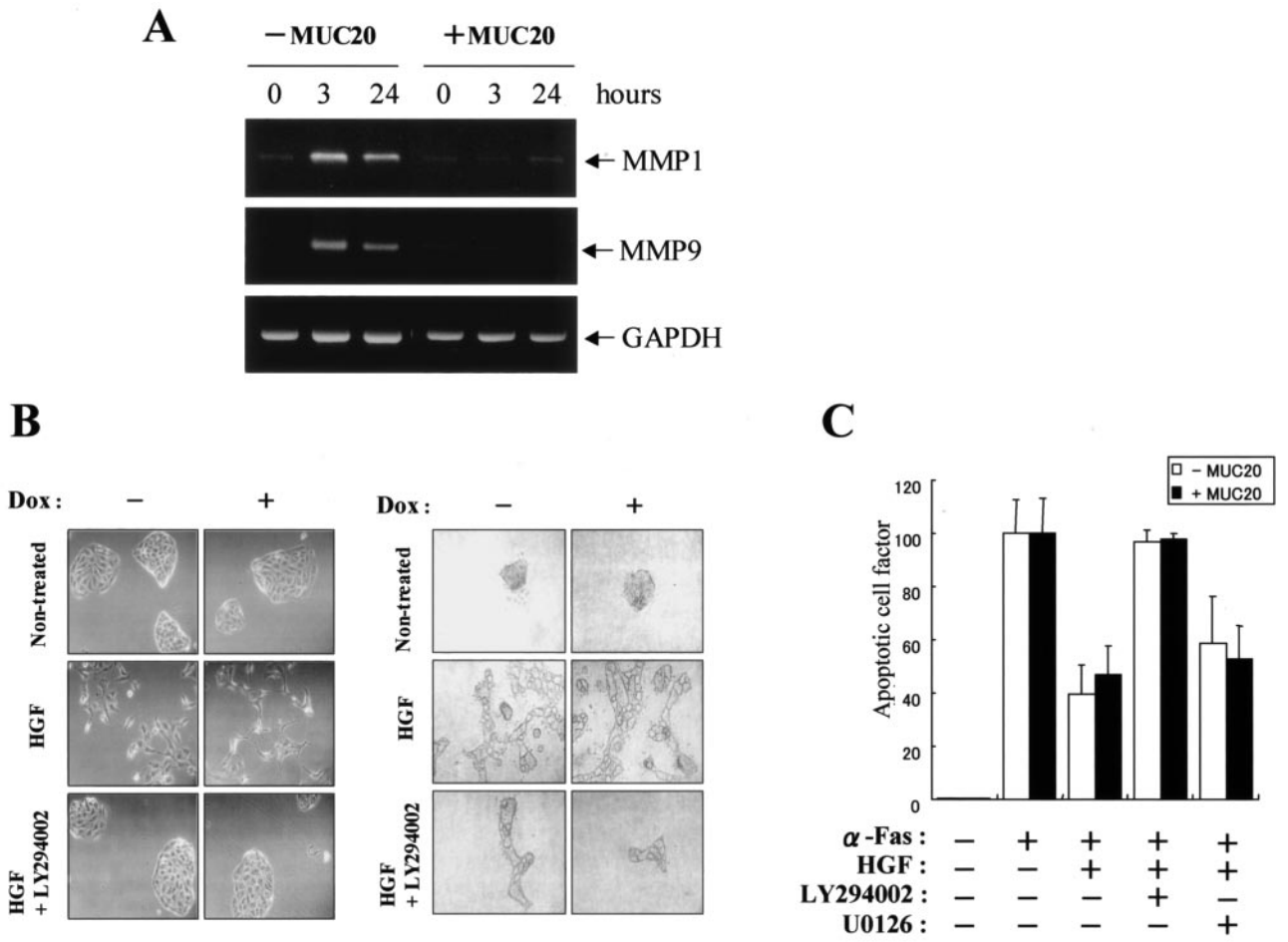

FIG. 3. Effects of MUC20 on HGF-induced biological responses. (A) RT-PCR analysis of MMP-1, MMP-9, and GAPDH mRNAs in HEK/*tet*-MUC20 cells at various times after HGF stimulation, with or without MUC20 production. (B) Left panels, micrographs showing cell dissociation and scatter of MDCK/*tet*-MUC20 cells with or without MUC20 production. The cells were pretreated with or without LY294002 prior to HGF stimulation. Right panels, phase-contrast micrographs of MDCK/*tet*-MUC20 cells with or without MUC20 production, grown in a three-dimensional collagen matrix. Cultures were maintained in the presence of HGF alone, HGF plus LY294002, or neither. (C) The antiapoptosis effect of HGF does not depend on MUC20 dose. HEK/*tet*-MUC20 cells with or without MUC20 production were pretreated with LY294002 or U0126 prior to HGF stimulation and then treated with an agonistic anti-Fas (α-Fas) antibody. Apoptosis was quantified by enzyme-linked immunosorbent assay for free nucleosomes. Results are represented as the ratio to apoptosis in the agonistic anti-Fas antibody-treated cells without HGF stimulation. Data represent mean ± standard deviations ($n = 3$).

malities up to 10 weeks of age under normal conditions. The primary cultures of the kidney proximal tubular cells from MUC20-Tg mice expressed 50-fold more MUC20 mRNA than those of non-Tg mice, even though Met mRNA levels were comparable in these cells (data not shown). HGF-induced phosphorylation of ERK1/2 in MUC20-Tg-derived cells was attenuated compared to that in non-Tg mice, whereas phosphorylation of Akt kinase, involved in the PI3K pathway, was not affected in these cells (Fig. 4A). As expected, HGF-elicited proliferation of the renal cells from MUC20-Tg mice was significantly impaired compared to that for non-Tg mice (Fig. 4B). We further examined the suppressive effect of MUC20 on liver cell proliferation evoked by exogenous hHGF in MUC20-Tg mice. A previous report showed that systemic administration of an hHGF expression plasmid (phHGF) by rapid injection led to high-level, sustained production of hHGF in mice (29). Since the expression of hHGF in vivo has been reported to promote liver cell proliferation and gain in liver weight, we tested whether MUC20 can suppress the hHGF-induced increase in liver weight. In non-Tg mice producing hHGF, the liver weights were markedly increased at 2 days after injection; however, those weight gains were significantly diminished in MUC20-Tg mice, indicating that MUC20 suppressed the hHGF-induced liver cell proliferation in vivo (Fig. 4C). To further validate the prediction that this suppressive effect was due to the binding of the DMB to Met, we cotransfected normal ICR mice with phHGF along with expression plasmids for either mouse MUC20 or MUC20[ΔC53]. Similar to the results observed in MUC20-Tg mice, HGF-induced gains in liver weight were reduced by production of MUC20; however, no reduction was found when the C-terminally truncated form was cointroduced, suggesting the importance of the DMB for suppression of HGF-induced liver cell proliferation (Fig. 4D). Combined, the results from in vitro

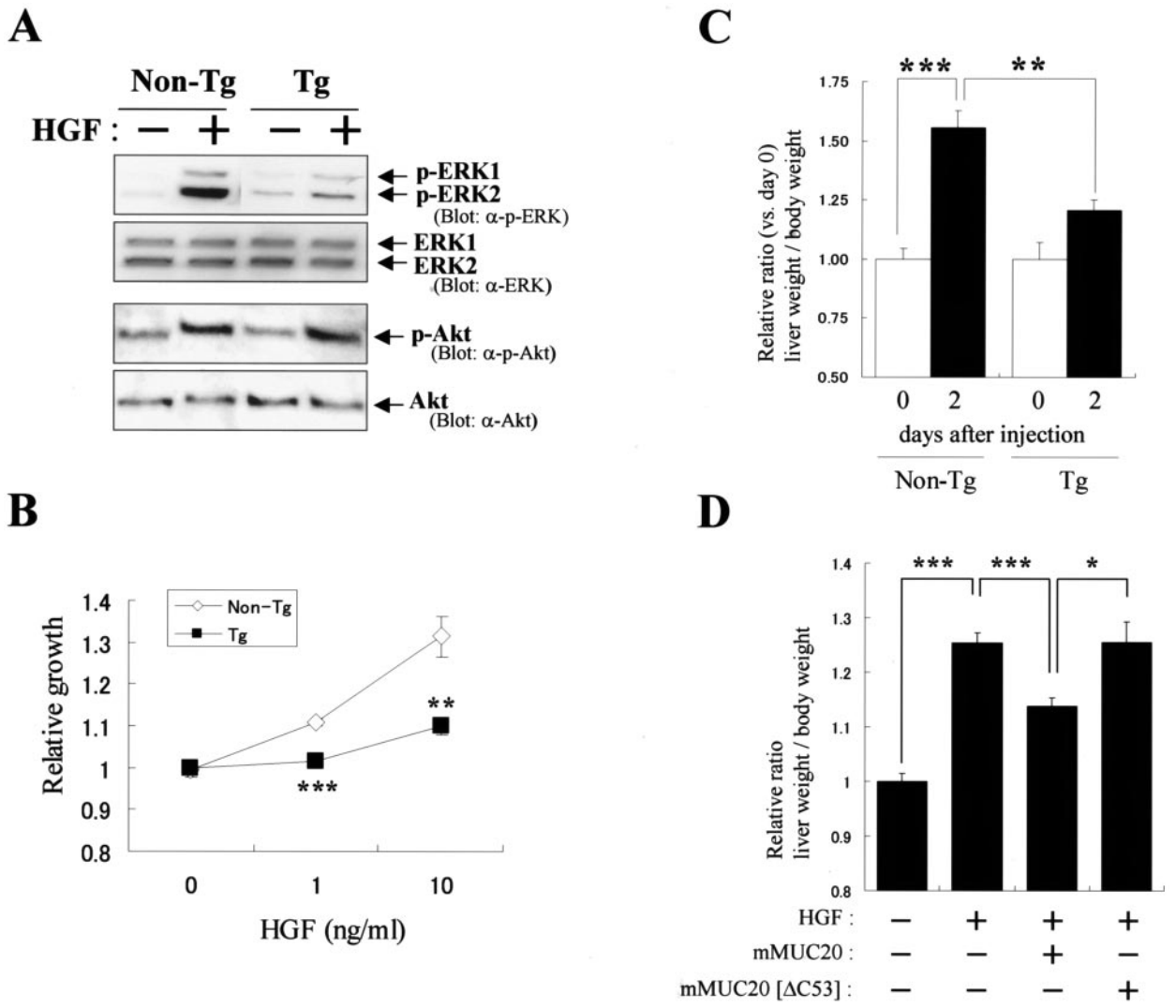

FIG. 4. MUC20 impairs HGF-induced proliferation. (A) Reduction of HGF-induced ERK1/2 phosphorylation by MUC20. Primary renal tubular cells from MUC20-Tg and non-Tg mice were stimulated with HGF, and the lysates were subjected to immunoblotting with the indicated antibodies (α-). (B) Attenuation of HGF-induced proliferation in primary cells from MUC20-Tg mice. Proliferation was measured by a cell viability assay. Data represent means ± standard deviations ($n = 3$). Similar results were obtained with primary cells from another strain of MUC20-Tg mice (data not shown). **, $P < 0.01$; ***, $P < 0.001$ (versus non-Tg mice in a two-tailed Student t test). (C) Attenuation of exogenous hHGF-induced liver weight gain in MUC20-Tg mice. The liver and body weights of the naked phHGF-injected mice were recorded at days 0 and 2. Data are presented as means ± standard deviations ($n = 6$). **, $P < 0.01$; ***, $P < 0.001$ (two-tailed Student t test). No differences in the amount of plasma hHGF were observed between non-Tg and Tg mice (1.56 ± 0.31 and 2.20 ± 1.29 ng/ml [means ± standard deviations], respectively [$n = 6$]). (D) Involvement of the DMB in suppression of the hHGF-induced liver weight gain. Either pmMUC20 or pmMUC20[ΔC53] was injected along with phHGF into ICR mice. No differences in the amount of plasma hHGF were observed among mice injected with phHGF alone, phHGF plus pmMUC20, or phHGF plus pmMUC20[ΔC53] (1.94 ± 0.92, 2.10 ± 0.95, and 1.64 ± 1.04 ng/ml [means ± standard deviations], respectively [$n = 6$]). The liver and body weights of these mice were recorded at day 2 after injection. Data are presented as means ± standard deviations ($n = 8$). *, $P < 0.05$; ***, $P < 0.001$ (two-tailed Student t test).

and in vivo experiments suggest that HGF-induced proliferation could be impaired due to the suppression of the Grb2-Ras pathway via the MUC20-Met binding.

MUC20 has a self-binding domain. In the search for MUC20-binding proteins in our two-hybrid screen with MUC[381-503] as a bait, we identified a 93-amino-acid peptide of the MUC20 C terminus, raising the possibility of MUC20 oligomerization. To confirm the oligomerization, Flag-tagged and poly(His)-tagged MUC20 coexpressed in HEK293 cells were tested for reciprocal coprecipitation by anti-Flag or anti-poly(His) antibodies. Figure 5A shows reciprocal immunoprecipitations with these antibodies, i.e., the presence of Flag-tagged MUC20 in the anti-poly(His) antibody precipitates and vice versa. To determine the region for the oligomerization, the self-binding abilities of several fragments within the cytoplasmic domain of MUC20 were evaluated in the two-hybrid assay. As shown in Fig. 5B, we detected self-binding of MUC[244-503], referred to as the whole cytoplasmic portion of MUC20, but no self-binding of the DMB, MUC[451-503]. The region responsible for the oligomerization seemed to be sep-

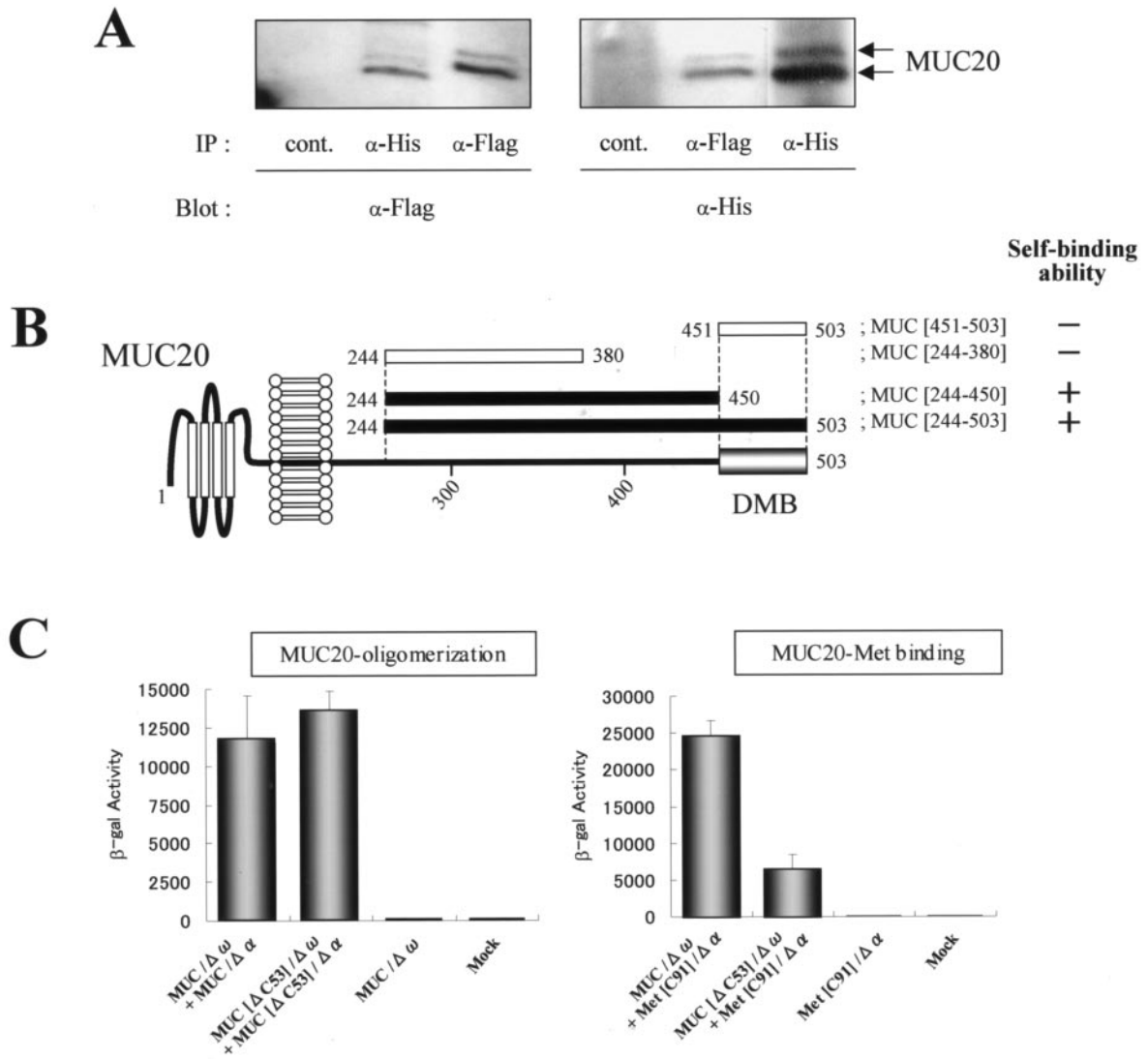

FIG. 5. MUC20 oligomerization domain. (A) Coimmunoprecipitation of tagged MUC20s. Lysates from HEK293 cells transfected with both phMUC20(Flag) and phMUC20(His) were subjected to immunoprecipitation (IP) and then to immunoblotting with the indicated antibodies (α-). (B) Determination of the region responsible for the oligomerization of MUC20. Self-binding and nonbinding abilities of each peptide in the two-hybrid assay are indicated as + and −, respectively. (C) β-Gal activities of CHO-K1 cells transfected with the chimeric constructs indicated below each bar. Data are represented as mean ± standard deviations ($n = 3$).

arate from but close to the DMB, because the self-binding ability of MUC[244-450] was eliminated by truncation of an additional 70 residues in MUC[244-380]. The region involved in MUC20 oligomerization was further dissected by using the β-Gal mutant system. In these experiments, we fused the Δω or Δα mutant with full-length MUC20 and with the DMB truncated form, resulting in MUC/Δω, MUC/Δα, MUC[ΔC53]/Δω, and MUC[ΔC53]/Δα. When the Δω and Δα fusions were coexpressed, the same level of β-Gal activity was generated by the full-length and the truncated MUC20 fusions, while the binding activity of MUC20 with Met (C-terminal 91 residues), assayed by coexpression of MUC/Δω and Met[C91]/Δα, was strongly diminished when MUC/Δω was replaced by MUC[ΔC53]/Δω (Fig. 5C). These results indicate that the cytoplasmic portion of MUC20 has two functional domains, one involved in MUC20 oligomerization and the other involved in MUC20-Met binding.

Binding to Met is augmented by MUC20 oligomerization. To better understand the relationship between the oligomerization and Met binding, we tested whether the Met binding could be promoted by the oligomerization by using three chimeric constructs, i.e., extracellular and transmembrane domains of Fas (eFas)/cytoplasmic portion of MUC20 (cMUC20), eFas/cMUC20/Δα, and eFas/cMUC20/Δω. First, using the β-Gal mutant system, we determined whether agonistic anti-Fas antibody gathering the eFas molecules enhances the association of the cMUC20 domains in eFas/cMUC20/Δα and eFas/cMUC20/Δω. As shown in Fig. 6A, the β-Gal activity in HEK293 cells coexpressing these constructs was increased by treatment with an agonistic antibody, RK-8, but not by

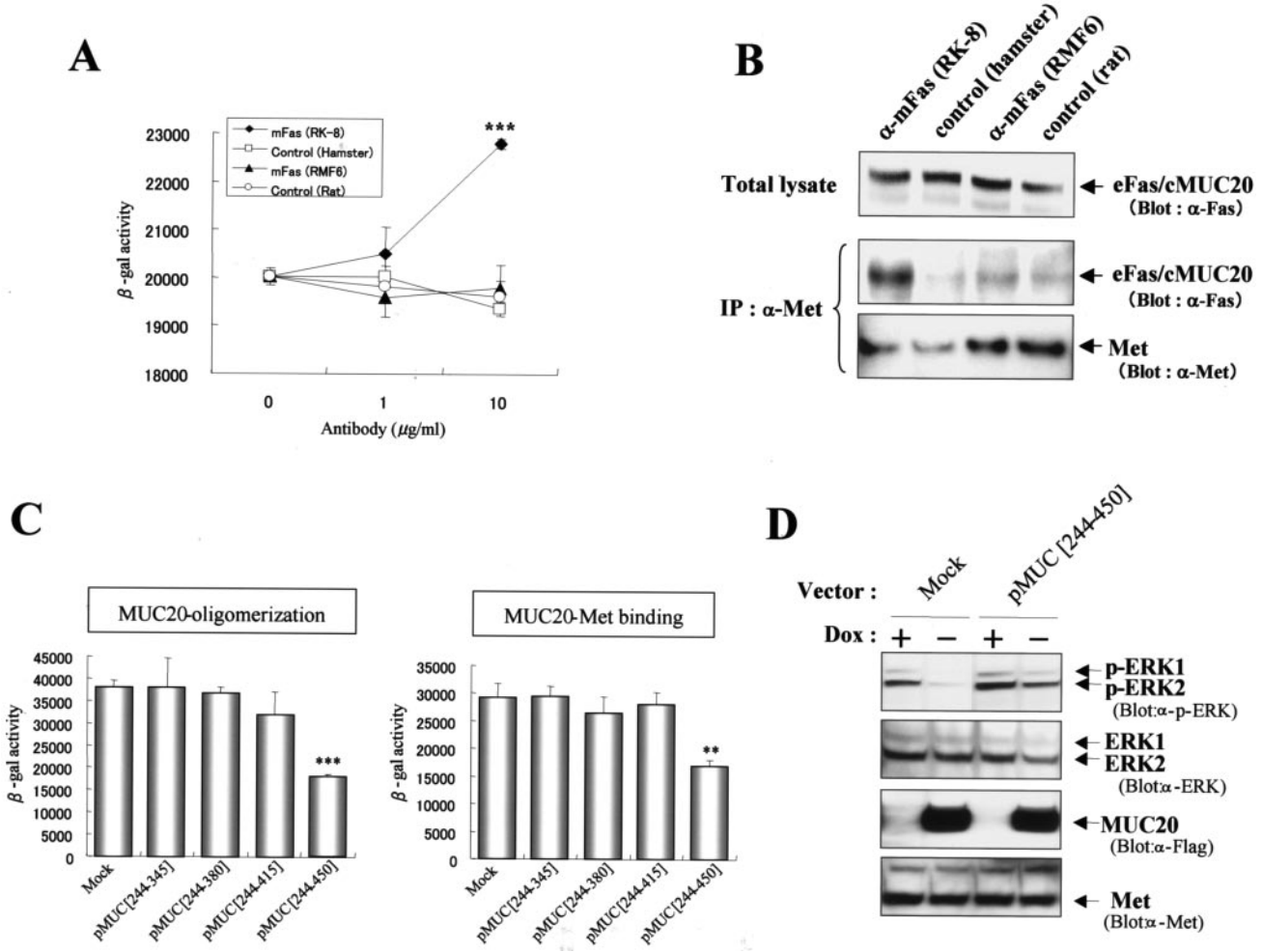

FIG. 6. Oligomerization of MUC20 augments its affinity to Met. (A) Oligomerization of the chimeric molecules by an agonistic anti-Fas antibody. HEK293 cells cotransfected with eFas/cMUC20/Δω and eFas/cMUC20/Δα were treated with anti-Fas (RK-8 or RMF6) or normal immunoglobulin G (control) antibodies, and then β-Gal activities were measured. Data are represented as mean ± standard deviations ($n = 3$). ***, $P < 0.001$ versus control in a two-tailed Student t test. (B) Augmentation of Met binding by oligomerization of the chimeric proteins. Immunoprecipitations (IP) with anti-Met (α-Met) antibody were performed with lysates from HEK293 cells expressing eFas/cMUC20. Cells were treated with the indicated antibodies for 3 h prior to preparation of the lysates. The precipitates were immunoblotted with the indicated antibodies. (C) Reduction of MUC20-Met binding by interference with MUC20 oligomerization. Each plasmid, pMUC[244-345], pMUC[244-380], pMUC[244-415], and pMUC[244-450], was transfected into CHO-K1 cells along with MUC/Δω plus MUC/Δα or MUC/Δω plus Met[C91]/Δα, and β-Gal activities were measured. Data are represented as means ± standard deviations ($n = 3$). **, $P < 0.01$; ***, $P < 0.001$ (versus mock transfectants in a two-tailed Student t test). (D) Release from suppression of the Grb2-Ras pathway by reduction of MUC20 oligomerization. pMUC[244-450] or pcDNA3 (Mock) was transfected into HEK/*tet*-MUC20 cells cultured in the presence or absence of DOX. After stimulation with HGF, the cell lysates were used for immunoblotting with the indicated antibodies.

treatment with RMF-6, a nonagonistic antibody (18), demonstrating that gathering of the Fas domains by agonistic antibodies leads to the clustering of the cytoplasmic portions of MUC20. Using these anti-Fas antibodies, we next tested whether the cytoplasmic oligomerization of MUC20 increases its affinity for Met. After treatment of cells expressing eFas/cMUC20 with the agonistic antibody, the amount of eFas/cMUC20 coimmunoprecipitated with Met was increased compared to that after treatment with other antibodies, implying that the affinity of MUC20 for Met could be augmented by oligomerization of MUC20 (Fig. 6B).

To gain further insight into the role of MUC20 oligomerization in the interaction with Met, expression vectors for the cytoplasmic portion of MUC20 were designed to test whether peptides that compete for MUC20 oligomerization would diminish the MUC20-Met binding. The effects of four peptides, produced by pMUC[244-345], pMUC[244-380], pMUC[244-415], and pMUC[244-450], on both oligomerization and Met binding were analyzed by using the β-Gal mutant system by cotransfection with each plasmid along with either MUC/Δω plus MUC/Δα or MUC/Δω plus Met[C91]/Δα. Of these plasmids, only pMUC[244-450], whose product was shown to have the self-binding domain (Fig. 5B), was able to reduce β-Gal activity in cells expressing MUC/Δω plus MUC/Δα, indicating that this peptide interfered with MUC20 oligomerization (Fig. 6C). MUC[244-450] also decreased β-Gal activity in cells expressing MUC/Δω plus Met[C91]/Δα, indicating reduced association between MUC20 and Met. To further test the possibil-

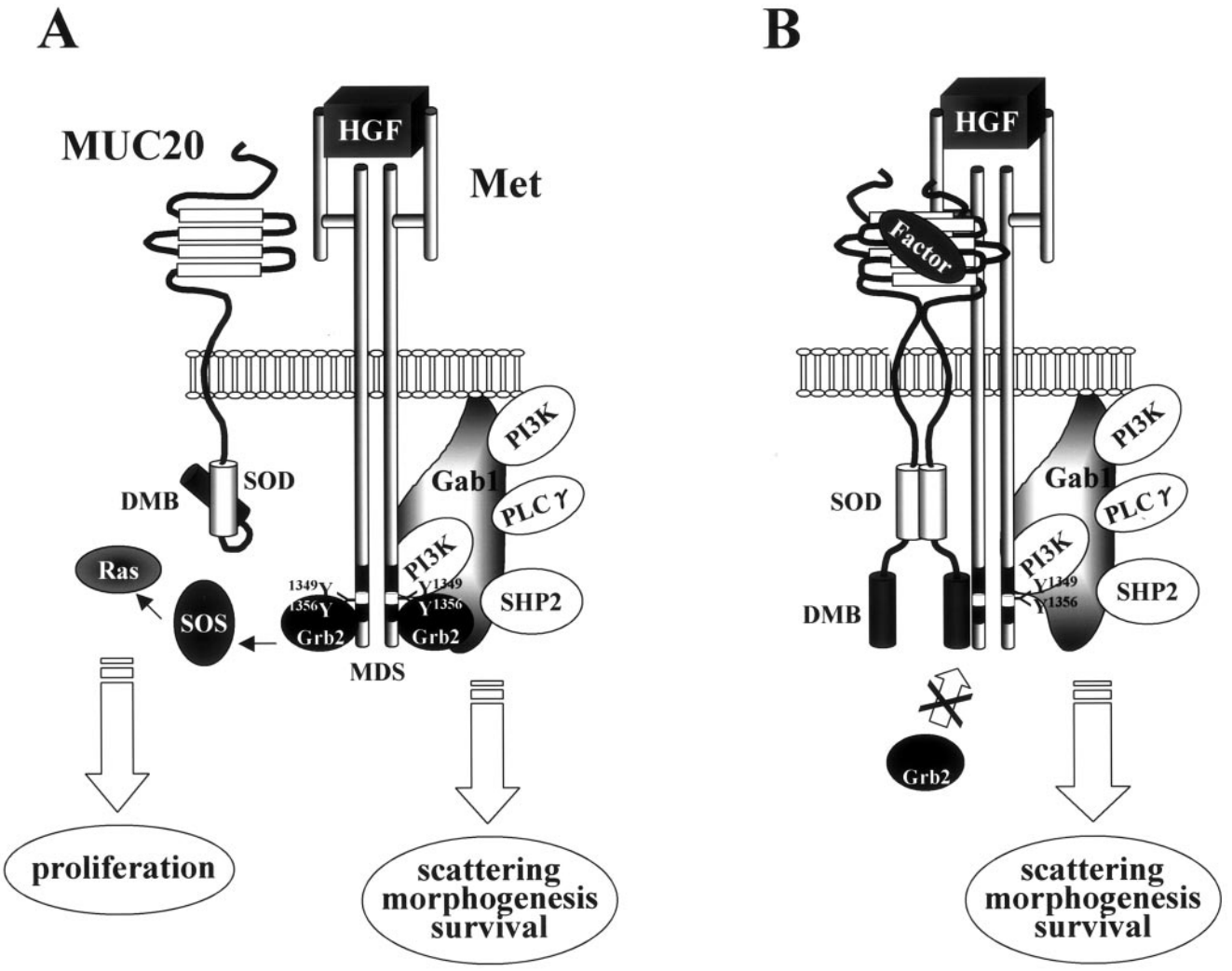

FIG. 7. Model of MUC20 suppression. (A) A MUC20 monomer has less ability to associate with Met. In this condition, Grb2 is recruited to HGF-activated Met, followed by activation of signaling cascades leading to proliferation. (B) MUC20 oligomerization caused by either an overproduction of MUC20 or an unknown endogenous factor(s) leads to the association with Met, blocking Grb2 recruitment to Met and suppressing the Grb2-Ras pathway, but does not affect Gab1 recruitment. The oligomerizing domain in MUC20 is referred to as the self-oligomerizing domain (SOD). PLCγ, phospholipase C-γ.

ity that interference with MUC20 oligomerization also interferes with the ability to suppress Met signaling, we examined whether the competitive peptide MUC[244-450] reduces the suppressive effect on HGF-induced ERK1/2 phosphorylation observed in MUC20-producing cells. As shown in Fig. 6D, this suppressive effect was effectively impaired by transfection with pMUC[244-450] compared to transfection of empty vector. Combined, these findings imply that the MUC20-Met binding is augmented by the oligomerization of MUC20.

DISCUSSION

The biological effects mediated by Met are controlled by concomitant activation of a number of signaling pathways. Prominent among these are the Grb2-Ras pathway eliciting transient activation of MAPK, which is required for proliferation, and the Gab1/PI3K pathways, which are required for cell scatter, morphogenesis, and cell survival (23). Recent reports have provided evidence that sustained MAPK activated the via Gab1 route (12, 25) is involved in the phenomena elicited by the latter pathways (1, 13). In this study, we found that MUC20 decreased HGF-induced transient MAPK activation through prevention of Grb2 recruitment, inhibiting HGF-induced proliferation and MMP expression. MUC20 did not, however, affect Gab1/PI3K pathways including the sustained MAPK activation, and consequently had no effect on cell scatter, branching morphogenesis, and cell survival (Fig. 7).

It is likely that the MUC20 binding does not cause drastic a structural change in Met, because dimerization and subsequent autophosphorylation of Met on HGF-stimulation occurred normally under MUC20-binding conditions. Recently, it was reported that a point mutation of Asn^{1358} in the MDS of Met causes a specific defect in Grb2 recruitment to Met (22). Although the defect might result from a conformational change in the MDS and thus may differ from the prevention of Grb2

recruitment by MUC20 binding, it is suggestive that the domain of Met required for MUC20 binding is near Asn^{1358} and may include the residue. Overproduction of MUC20 was needed to detect the Met binding; thus, the binding affinity might be rather low, even if oligomerization has made the conformation of MUC20 favorable for Met binding. Grb2 is a small protein that binds to the $Y^{1356}VNV$ sequence in the MDS, while Gab1 is a larger molecule that binds Met directly via Y^{1349} and indirectly via a Grb2 linkage. Recently, the C-terminal lobe of the Met kinase domain also was found to be involved in direct Gab1 binding (11), suggesting that extended regions of Met might be involved in the Gab1 binding. Thus, we propose that the selective prevention of the Grb2 recruitment is caused by low-affinity attachment of MUC20 to a restricted area possibly around $Y^{1356}VNV$ in the MDS, and that the Gab1 interaction is not affected due to higher-affinity binding to Met.

To gain insight into the physiological role of Grb2 recruitment to Met, mutant mice that produce Met with a point mutation to eliminate the Grb2-binding site have been generated (7). These mice were viable but showed abnormality of postnatal cerebellar development. MUC20-Tg mice, in contrast, had no apparent phenotypic abnormalities, although we expected hypomorphological phenotypes of the tissues, due to the reduction of HGF-dependent proliferation. These results raise the possibility that the Grb2 recruitment to Met may not be required during development. In general, the Grb2-Ras pathway is a crucial common pathway that is responsible for promoting proliferation. Therefore, the down-regulation of this pathway in Met signaling might be compensated promptly by the action of other factors, e.g., EGF and fibroblast growth factor, during development. Our proposal for the physiological role of MUC20 is not only a suppression of HGF-induced proliferation but also an emphasizing of morphological stimuli of HGF. Namely, in kidney, after HGF provides a proliferative stimulus to the dedifferentiated cells, the effect of HGF on those cells could be switched to a morphogenesis stimulus by MUC20 through suppression of the Grb2-Ras pathway, leading to successful generation of renal tubules. Indeed, we observed that in mouse renal tissues injured by cisplatin, the expression of MUC20 mRNA was increased in parallel with an increase in blood urea nitrogen, a marker of renal damage, and then was returned to the normal level until the regeneration was completed (6), whereas HGF was markedly and rapidly produced once treatment for acute renal injury was given (8).

Besides recruitment of PI3K, Gab1, and Grb2, Met is also known to interact with FAP68 and RanBPM. FAP68 binds specifically to the inactive form of Met and is released upon Met phosphorylation (5). Paradoxically, RanBPM interacts with Met regardless of HGF stimulation, but the interaction is enhanced by HGF (27). In this study, we demonstrated that MUC20 binding to Met is independent of HGF stimulation and that the interaction tends to be strengthened by MUC20 oligomerization. Previous reports have shown that extracellular regions of mucin-type glycoproteins are able to interact with bacteria or distinct ligands, such as L- and P-selectins, and play important roles in protective functions and cell adhesion. Thus, we further propose a novel paradigm through which endogenous factors that are not ligand molecules for a growth factor receptor may be able to regulate signal transduction of the growth factor by inducing a conformation change in its recognizing proteins, e.g., mucin-type glycoproteins.

Previous studies have demonstrated that another transmembrane mucin, MUC1, interacts with the EGF receptor, and activation of EGF receptor leads to phosphorylation of MUC1 (10). Moreover, the MUC1 phosphorylation enhances c-Src and β-catenin recruitment and modulation of EGF-induced ERK1/2 activation (26). Recently, HGF stimulation was found to increase phosphorylation of MUC20. This phenomenon is likely to be mediated by the Gab1/PI3K pathways, because the phosphorylation of MUC20 upon stimulation with HGF was markedly reduced by LY294002 but not by U0126 (unpublished data). Although the role of MUC20 phosphorylation has not yet been established, we propose that this modification did not affect the binding ability of MUC20 to Met within 30 min after HGF stimulation (Fig. 1A) and that the HGF-induced phosphorylation might serve as an important regulator of events downstream of HGF signaling.

In summary, we have carried out functional analyses of MUC20 and have demonstrated that it is a novel negative regulator of the HGF-induced Grb2-Ras pathway. The Met signaling cascade is believed to serve important roles in cell growth and differentiation, organ regeneration, and tumorigenesis. Tight regulation of this system could be required for control of essential actions of HGF. HGF is considered to be a possible therapeutic agent, as it displays a remarkable ability to ameliorate renal injury and fibrosis by enhancing cell survival and tissue regeneration in acute and chronic disease conditions. Factors that regulate MUC20 expression and/or function may be useful therapeutics for the development and progression of renal diseases.

ACKNOWLEDGMENTS

We thank T. Chuman, K. Iwata, H. Sasai, H. Ogasawara, and M. Sasabuchi (JT Pharma); E. Imai (Osaka University); W. Munger (Gene Logic Inc.); and R. Falk, C. Jennette, and D. Alcorta (University of North Carolina) for discussion and H. Murakoshi, I. Suganuma, K. Ishii, M. Saito, S. Kubo, Y. Mohara, and N. Ookawara (JTCS) for technical assistance. We also thank J. Miyazaki (Osaka University) for the vector pCAGGS.

REFERENCES

1. **Boccaccio, C., M. Ando', and P. M. Comoglio.** 2002. A differentiation switch for genetically modified hepatocytes. FASEB J. **16:**120–122.
2. **Comoglio, P. M., and C. Boccaccio.** 1996. The HGF receptor family: unconventional signal transducers for invasive cell growth. Genes Cells **1:**347–354.
3. **Di Renzo, M. F., R. P. Narsimhan, M. Olivero, S. Bretti, S. Giordano, E. Medico, P. Gaglia, P. Zara, and P. M. Comoglio.** 1991. Expression of the Met/HGF receptor in normal and neoplastic human tissues. Oncogene **6:**1997–2003.
4. **Gandino, L., P. Longati, E. Medico, M. Prat, and P. M. Comoglio.** 1994. Phosphorylation of serine 985 negatively regulates the hepatocyte growth factor receptor kinase. J. Biol. Chem. **269:**1815–1820.
5. **Grisendi, S., B. Chambraud, I. Gout, P. M. Comoglio, and T. Crepaldi.** 2001. Ligand-regulated binding of FAP68 to the hepatocyte growth factor receptor. J. Biol. Chem. **276:**46632–46638.
6. **Higuchi, T., T. Orita, S. Nakanishi, K. Katsuya, H. Watanabe, Y. Yamasaki, I. Waga, T. Nanayama, Y. Yamamoto, W. Munger, H-W. Sun, R. J. Falk, J. C. Jennette, D. A. Alcorta, H. Li, T. Yamamoto, Y. Saito, and M. Nakamura.** 2004. Molecular cloning, genomic structure and expression analysis of MUC20, a novel mucin protein, up-regulated in injured kidney. J. Biol. Chem. **279:**1968–1979.
7. **Ieraci, A., P. E. Forni, and C. Ponzetto.** 2002. Viable hypomorphic signaling mutant of the Met receptor reveals a role for hepatocyte growth factor in postnatal cerebellar development. Proc. Natl. Acad. Sci. USA **99:**15200–15205.
8. **Igawa. T., K. Matsumoto, S. Kanda, Y. Saito, and T. Nakamura.** 1993. Hepatocyte growth factor may function as a renotropic factor for regeneration in rats with acute renal injury. Am. J. Physiol. **265:**F61–F69.

9. **Khwaja, A., K. Lehmann, B. M. Marte, and J. Downward.** 1998. Phosphoinositide 3-kinase induces scattering and tubulogenesis in epithelial cells through a novel pathway. J. Biol. Chem. **273:**18793–18801.
10. **Li, Y., J. Ren, W. Yu, Q. Li, H. Kuwahara, L. Yin, K. L. Carraway, and D. Kufe.** 2001. The epidermal growth factor receptor regulates interaction of the human DF3/MUC1 carcinoma antigen with c-Src and beta-catenin. J. Biol. Chem. **276:**35239–35242.
11. **Lock, L. S., M. M. Frigault, C. Saucier, and M. Park.** 2003. Grb2-independent recruitment of Gab1 requires the C-terminal lobe and structural integrity of the Met receptor kinase domain. J. Biol. Chem. **278:**30083–30090.
12. **Maroun, C. R., M. A. Naujokas, M. Holgado-Madruga, A. J. Wong, and M. Park.** 2000. The tyrosine phosphatase SHP2 is required for sustained activation of extracellular signal-regulated kinase and epithelial morphogenesis downstream from the Met receptor tyrosine kinase. Mol. Cell. Biol. **20:**8513–8525.
13. **Marshall, C. J.** 1995. Specificity of receptor tyrosine kinase signaling: transient versus sustained extracellular signal-regulated kinase activation. Cell **80:**179–185.
14. **Menaa, C., F. Vrtovsnik, G. Friedlander, M. Corvol, and M. Garabedian.** 1995. Insulin-like growth factor I, a unique calcium-dependent stimulator of 1,25-dihydroxyvitamin D3 production. Studies in cultured mouse kidney cells. J. Biol. Chem. **270:**25461–25467.
15. **Miller, S. B., D. R. Martin, J. Kissane, and M. R. Hammerman.** 1994. Hepatocyte growth factor accelerates recovery from acute ischemic renal injury in rats. Am. J. Physiol. **266:**F129–F134.
16. **Mizuno, S., K. Matsumoto, T. Kurosawa, Y. Mizuno-Horikawa, and T. Nakamura.** 2000. Reciprocal balance of hepatocyte growth factor and transforming growth factor-beta 1 in renal fibrosis in mice. Kidney Int. **57:**937–948.
17. **Mizuno, S., K. Matsumoto, and T. Nakamura.** 2001. Hepatocyte growth factor suppresses interstitial fibrosis in a mouse model of obstructive nephropathy. Kidney Int. **59:**1304–1314.
18. **Nishimura, Y., A. Ishii, Y. Kobayashi, Y. Yamasaki, and S. Yonehara.** 1995. Expression and function of mouse Fas antigen on immature and mature T cells. J. Immunol. **154:**4395–4403.
19. **Niwa, H., K. Yamamura, and J. Miyazaki.** 1991. Efficient selection for high-expression transfectants with a novel eukaryotic vector. Gene **108:**193–199.
20. **Peschard, P., T. M. Fournier, L. Lamorte, M. A. Naujokas, H. Band, W. Y. Langdon, and M. Park.** 2001. Mutation of the c-Cbl TKB domain binding site on the Met receptor tyrosine kinase converts it into a transforming protein. Mol. Cell **8:**995–1004.
21. **Petrelli, A., G. F. Gilestro, S. Lanzardo, P. M. Comoglio, N. Migone, and S. Giordano.** 2002. The endophilin-CIN85-Cbl complex mediates ligand-dependent downregulation of c-Met. Nature **416:**187–190.
22. **Ponzetto, C., Z. Zhen, E. Audero, F. Maina, A. Bardelli, M. L. Basile, S. Giordano, R. Narsimhan, and P. M. Comoglio.** 1996. Specific uncoupling of Grb2 from the Met receptor. J. Biol. Chem. **271:**14119–14123.
23. **Rosário, M., and W. Birchmeier.** 2003. How to make tubes: signaling by the Met receptor tyrosine kinase. Trends Cell Biol. **13:**328–335.
24. **Rossi, F., C. A. Charlton, and H. M. Blau.** 1997. Monitoring protein-protein interactions in intact eukaryotic cells by beta-galactosidase complementation. Proc. Natl. Acad. Sci. USA **94:**8405–8410.
25. **Schaeper, U., N. H. Gehring, K. P. Fuchs, M. Sachs, B. Kempkes, and W. Birchmeier.** 2000. Coupling of Gab1 to c-Met, Grb2, and Shp2 mediates biological responses. J. Cell Biol. **149:**1419–1432.
26. **Schroeder, J. A., M. C. Thompson, M. M. Gardner, and S. J. Gendler.** 2001. Transgenic MUC1 interacts with epidermal growth factor receptor and correlates with mitogen-activated protein kinase activation in the mouse mammary gland. J. Biol. Chem. **276:**13057–13064.
27. **Wang, D., Z. Li, E. M. Messing, and G. Wu.** 2002. Activation of Ras/Erk pathway by a novel MET-interacting protein RanBPM. J. Biol. Chem. **277:** 36216–36222.
28. **Xiao, G. H., M. Jeffers, A. Bellacosa, Y. Mitsuuchi, G. F. V. Woude, and J. R. Testa.** 2001. Anti-apoptotic signaling by hepatocyte growth factor/Met via the phosphatidylinositol 3-kinase/Akt and mitogen-activated protein kinase pathways. Proc. Natl. Acad. Sci. USA **98:**247–252.
29. **Yang, J., S. Chen, L. Huang, G. K. Michalopoulos, and Y. Liu.** 2001. Sustained expression of naked plasmid DNA encoding hepatocyte growth factor in mice promotes liver and overall body growth. Hepatology **33:**848–859.
30. **Zeigler, M. E., Y. Chi, T. Schmidt, and J. Varani.** 1999. Role of ERK and JNK pathways in regulating cell motility and matrix metalloproteinase 9 production in growth factor-stimulated human epidermal keratinocytes. J. Cell Physiol. **180:**271–284.